ACS APPLIED MATERIALS & INTERFACES

Research Article

www.acsami.org

Surface-Initiated Hyperbranched Polyglycerol as an Ultralow-Fouling Coating on Glass, Silicon, and Porous Silicon Substrates

Eli Moore,[†,‡] Bahman Delalat,[†] Roshan Vasani,[†] Gordon McPhee,[†] Helmut Thissen,[‡] and Nicolas H. Voelcker*[,†]

[†]ARC Centre of Excellence in Convergent Bio-Nano Science and Technology, Mawson Institute, University of South Australia, GPO Box 2471, Adelaide, South Australia 5001, Australia

[‡]CSIRO Materials Science and Engineering, Bayview Avenue, Clayton, Victoria 3168, Australia

Supporting Information

ABSTRACT: Anionic ring-opening polymerization of glycidol was initiated from activated glass, silicon, and porous silicon substrates to yield thin, ultralow-fouling hyperbranched polyglycerol (HPG) graft polymer coatings. Substrates were activated by deprotonation of surface-bound silanol functionalities. HPG polymerization was initiated upon the addition of freshly distilled glycidol to yield films in the nanometer thickness range. X-ray photoelectron spectroscopy, contact angle measurements, and ellipsometry were used to characterize the resulting coatings. The antifouling properties of HPG-coated surfaces were evaluated in terms of protein adsorption and the attachment of mammalian cells. The adsorption of bovine serum albumin and collagen type I was found to be reduced by as much as 97 and 91%, respectively, in comparison to untreated surfaces. Human glioblastoma and mouse fibroblast attachment was reduced by 99 and 98%, respectively. HPG-grafted substrates outperformed polyethylene glycol (PEG) grafted substrates of comparable thickness under the same incubation conditions. Our results demonstrate the effectiveness of antifouling HPG graft polymer coatings on a selected range of substrate materials and open the door for their use in biomedical applications.

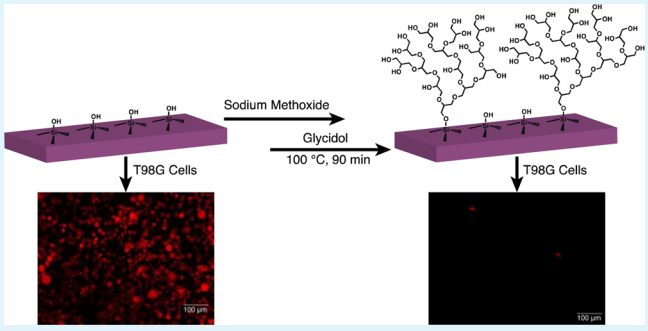

KEYWORDS: *hyperbranched polyglycerol, surface grafting, biofouling, antifouling, low-fouling, nonfouling*

INTRODUCTION

Antifouling surfaces that are resistant to protein and cell adhesion are of crucial importance in the fields of biotechnology and biomedicine.[1,2] Biofouling is an issue that plagues many modern products and practices in the medical and scientific communities. Products such as implantable medical devices, catheters, and contact lenses, along with cell culture substrates and immunoassays, just to name a few, all rely on a level of protection against biofouling.[3−8] Issues such as infection around an implant can be caused by biofouling on the surface of the implanted device.[9] In contrast, an implant with a suitable antifouling coating can avoid biofouling and prevent infections. Currently, the industry standard in polymeric antifouling coatings are polyethylene glycol (PEG) graft polymers.[10,11] Extensive research has been carried out on the grafting of linear PEG in order to produce antifouling coatings.[12−15] Besides the grafting of linear PEG, other PEG architectures such as star-PEG hydrogels and surface initiated PEG brushes have been investigated, with the resulting films displaying excellent antifouling properties.[16−18] However, even with the emergence of new PEG architectures, limitations such as oxidative degradation and limited functionality leave ample room for improvement over PEG.[7]

Hyperbranched polyglycerol (HPG) is chemically analogous to PEG except it is in a hyperbranched globular form.[19] In contrast to linear PEG, HPGs have an abundance of terminal functional groups that are advantageous for further functionalization.[20,21] Furthermore, it has been demonstrated that HPGs possess greater thermal and oxidative stability over PEG.[22] This provides an added benefit in medical applications where thermal sterilization is often required or when the device is implanted and oxidative degradation of the PEG coating is a known issue.[23] Therefore, HPGs have the potential to replace PEGs across a range of applications if suitable grafting techniques can be developed. Previously, HPG coatings produced via grafting-to approaches to various substrates have been studied for their resistance to protein adsorption as well as cell and bacterial attachment.[24,25] These techniques have traditionally required multistep modifications of the HPGs to allow for surface attachment. The most common of those is thiol modification, which allows self-assembled monolayer formation on gold via a gold−thiol bond.[22,26,27] While these

Received: June 5, 2014
Accepted: August 19, 2014
Published: August 19, 2014

techniques were generally able to exhibit degrees of resistance comparable with the industry standard PEG, results were inconsistent as it proved difficult to overcome defect sites across the surface. Due to the nature of the grafting-to techniques and the globular structure of HPGs, voids were inevitably left in the monolayer structure that became sites for nonspecific attachment of unwanted species.[28] Unfortunately, uniform layers of HPGs are difficult to achieve due to steric hindrance of the globular molecules, preventing high-density grafting. In contrast, it stands to reason that by employing the grafting-from approach, both grafting density and film thickness could be optimized to achieve superior antifouling properties.[29] The inherent limitations of grafting-to techniques are not restricted to larger globular polymers such as HPGs. Surface-initiated grafting techniques have also been investigated for other polymeric antifouling surface coatings, including PEG, in an effort to increase grafting density and thickness and to improve surface coverage.[30,31]

Here, we investigate the antifouling properties of high-density HPG graft polymer surfaces produced via the grafting-from approach. The anionic ring-opening polymerization of glycidol can be initiated from surface-bound silanol functionalities following deprotonation.[32] Therefore, glass, single-crystal silicon wafer and biodegradable porous silicon (pSi) substrates were studied due to the availability of silicon oxide at the surface of each substrate, along with popularity of these substrates in the biomedical field. Immunoassays and in vitro diagnostics are routinely carried out on glass microscope slides, making the availability of antifouling glass coatings highly desirable. Furthermore, due to their optical and physical properties, silicon and pSi are emerging as interesting substrates for many biosensing and biomedical applications.[33,34] The addition of an antifouling graft polymer coating to these substrates, in the form of HPG, provides an opportunity to further their development into biomedical applications, particularly where a high level of antifouling behavior is required. The surface-initiated polymerization of glycidol from glass, silicon, and pSi surfaces was tailored to optimize antifouling properties against proteins and anchorage-dependent cells. These surfaces proved to be ultralow-fouling in our hands and outperformed linear PEG-grafted substrates of comparable film thickness prepared under optimized cloud-point conditions.[35]

MATERIALS AND METHODS

Glycidol (Sigma, 96%) was distilled under vacuum and stored over molecular sieves in the freezer overnight. Glass microscope slides (Menzel-Gläser, 76 × 26 mm^2) were cut and washed with ethanol prior to use. P-type silicon wafers (Siegert Wafer; Boron doped; ⟨100⟩ orientation; ≲3 Ω cm; 381 μm) were cut and washed with acetone and dichloromethane and dried under a stream of N_2 gas prior to use. Hydrofluoric acid (Chemsupply, 48% in water) was diluted 1:1 in ethanol. Methanol (Chemsupply, 100% undenatured) and 1,4-dioxane (Sigma, 99%) were dried over molecular sieves before use. Toluene (Sigma, 98%) was distilled from sodium metal and benzophenone (Sigma, 99%) under N_2 and stored over molecular sieves. Sodium metal (Sigma, ≥99%, stored under mineral oil) was washed in hexane after weighing. Albumin from bovine serum (BSA, Sigma, ≥96%) and collagen type I (Sigma) were made up into stock solutions of 100 μg/mL in phosphate buffered saline (Sigma, PBS, pH 7). PEG bis(amine) (Sigma, 3,000 MW) and (3-glycidyloxypropyl)trimethoxysilane (Sigma, ≥98%) were used as received.

For cell culture, the following reagents were used: 0.01 M PBS pH 7.4, paraformaldehyde solution (4%, Electron Microscopy Science). Dulbecco's modified Eagle medium (DMEM, Invitrogen), fetal bovine serum (FBS, Invitrogen), L-glutamine (Invitrogen), penicillin (Invitrogen), streptomycin (Invitrogen), amphotericin B (Invitrogen), CellTracker Orange (Invitrogen), propidium iodide (PI, Sigma), fluorescein diacetate (FDA, Sigma), Fluoro-Gel mounting medium (ProSciTech), and trypsin (0.05%, EDTA 0.53 mM, Life Technologies) were all used as received. All incubation took place at room temperature unless otherwise stated. All solutions were prepared using ultrapure water obtained from a Milli-Q system (Millipore). NIH/3T3, mouse embryonic fibroblast cells ATCC CRL-1658 (American Type Culture Collection, Manassas, VA) and T98G human glioblastoma cells (ATCC CRL-1690) were used in the experiments.

Contact Angle Measurements. Milli-Q water (18.2 MΩ cm, 3 μL) was placed onto the samples using a 100 μL Hamilton syringe fitted with a hydrophobic sleeve, and images were captured using a Panasonic WV-BP550/G CCTV camera. The static contact angle was measured using ImageJ software with the drop analysis plugin. All measurements were repeated a minimum of three times, and the results were averaged.

X-ray Photoelectron Spectroscopy (XPS). XPS was performed using an AXIS Ultra DLD spectrometer (Kratos Analytical Inc., Manchester, U.K.) with a monochromated Al Kα source at a power of 45 W (15 kV, 3 mA), a hemispherical analyzer operating in the fixed analyzer transmission mode, and the standard aperture (1 × 0.5 mm^2 slot). The total pressure in the main vacuum chamber during analysis was typically 10^{-8} mbar. Each specimen was analyzed at an emission angle of 0° as measured from the surface normal. Assuming typical values for the electron attenuation length of relevant photoelectrons in organic compounds, the XPS analysis depth (from which 95% of the detected signal originates) ranges between 5 and 10 nm. An elliptical area with approximately dimensions of 0.3 × 0.7 mm^2 was analyzed on each sample.

Data processing was performed using CasaXPS processing software version 2.3.15 (Casa Software Ltd., Teignmouth, U.K.). All elements present were identified from survey spectra (acquired at a pass energy of 160 eV). To obtain more detailed information, we recorded high-resolution spectra from individual peaks at 40 eV pass energy (yielding a typical peak width for polymers of 1.0−1.1 eV). These data were quantified using a Simplex algorithm to calculate optimized curve fits and thus to determine the contributions from specific functional groups. The atomic concentrations of the detected elements were calculated using integral peak intensities and the sensitivity factors supplied by the manufacturer. Binding energies were referenced to the aliphatic hydrocarbon peak at 285.0 eV.

Scanning Electron Microscopy (SEM). SEM imaging and characterization was conducted on a Quanta 450 FEG Environmental SEM (FEI, Netherlands) fitted with an SSD detector and operated at 30 kV.

Ellipsometry. The thickness of grafted HPG films were measured with a J.A. Woollam V-Vase ellipsometer using wavelengths between 250 and 1100 nm in 10 nm increments and at 65, 70, and 75° from the surface normal. To obtain the ellipsometric thickness of the grafted HPG films, we fitted the VASE spectra with the multilayer model on the basis of the WVASE32 analysis software, using the optical properties of a generalized Cauchy layer.

Fluorescence Microscopy Imaging. Fluorescence microscopy images were captured using Nikon Eclipse-TiS microscope fitted with a Nikon Digital Sight DS-2MBWc digital camera head and Nikon NIS-Elements imaging software.

Atomic Force Microscopy (AFM). AFM imaging was performed using a NanoWizard III BioAFM (JPK Instruments, Berlin). The images (5 × 5 μm) were recorded in air and pure water at 22 °C in contact mode. The probes used were FORT (AppNano) with a spring constant in the range of 1.2−6.4 N/m (manufacturer's values).

Preparation of HPG-Grafted Flat Silicon and Glass Substrates. Freshly distilled glycidol was polymerized directly from flat silicon and glass substrates using procedures first developed by Huck et al.[32] In short, silicon wafer and glass microscope slides were cut into 1 cm^2 pieces, washed with ethanol, and dried under a stream of N_2. The substrates were treated with a mixture of ammonium hydroxide, hydrogen peroxide, and Milli-Q water in a ratio of 1:1:5 (also known

Scheme 1. Proposed Growth Mechanism for Surface-Initiated HPG Synthesis from Oxidised Silicon and Glass Substrates

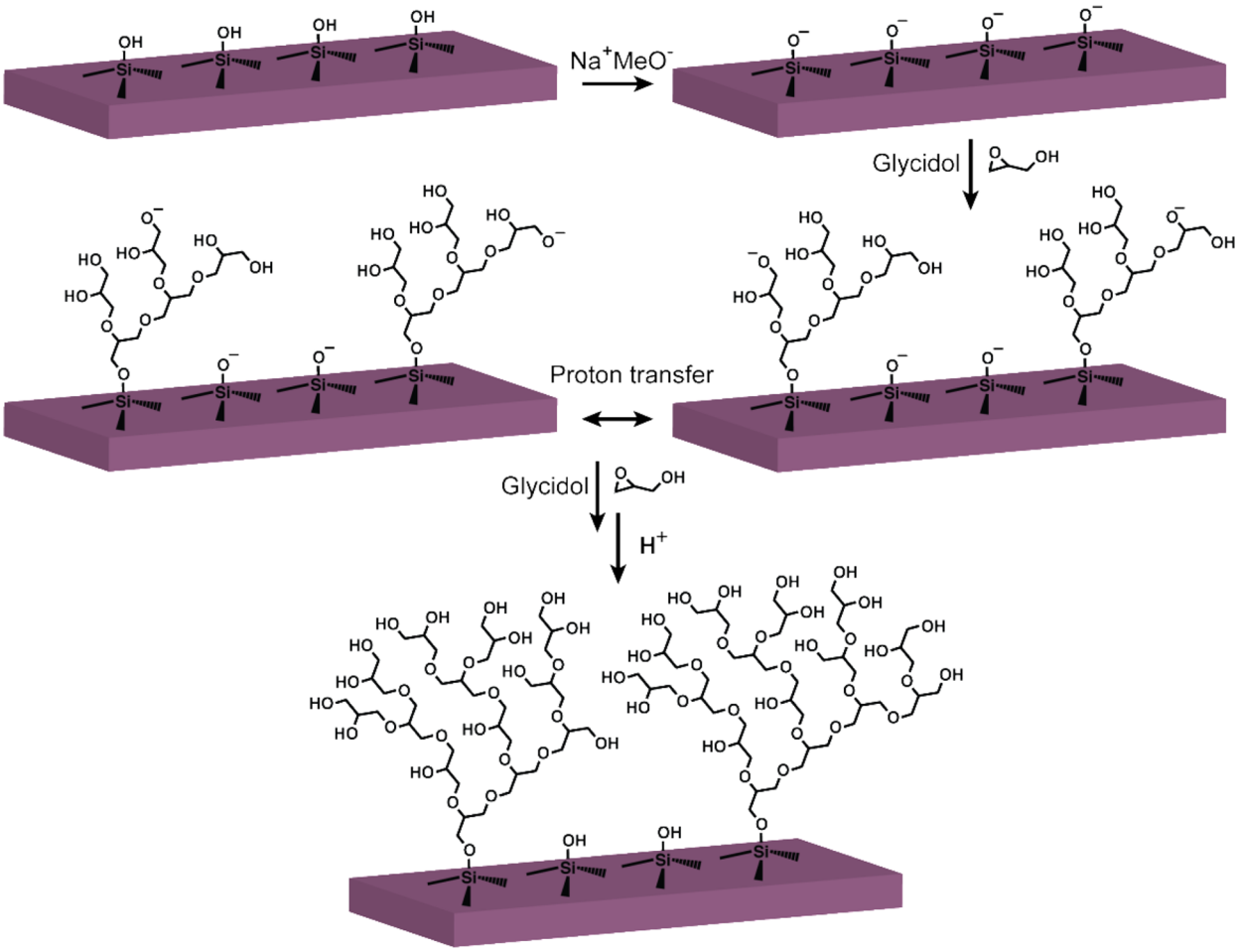

as RCA cleaning) at 70 °C for 30 min; washed with water and ethanol; and dried under a stream of N_2. Sodium methoxide in methanol (10 mL, 0.15 M) was added to the substrates under N_2 at 70 °C, and after 1 h, the solution was removed, and the substrates were washed thoroughly with methanol (anhydrous, 3 × 20 mL) and toluene (anhydrous, 3 × 30 mL) using a syringe. The substrates were dried under vacuum at 100 °C for 20 min, and glycidol (distilled the day before and dried over molecular sieves for 18 h) was added to cover the substrates. After 90 min at 100 °C under N_2, the unreacted monomer was removed and water was added. The resulting HPG-grafted substrates were washed thoroughly with water and ethanol and dried under a stream of N_2.

Preparation of Porous Silicon. Porous silicon (pSi) was prepared using a wet electrochemical approach such that an average pore size of 20 nm diameter was obtained.[36] The cleaned wafer pieces were placed into a Teflon etching cell with an exposed area of 1.76 cm^2. The cell was filled with a mixture containing 24% aqueous hydrofluoric acid in ethanol, which acted as the electrolyte and etchant. The silicon wafer piece was placed on a piece of aluminum foil, and together they acted as the anode, while a platinum mesh placed parallel to the surface acted as the cathode. The electrochemical anodization was performed at a current density of 5.7 mA/cm^2 for 900 s using a Keithley 2425 source meter. Following the etching, the surface was washed with methanol, ethanol, acetone, and dichloromethane in series and then dried under a stream of N_2 gas. Prior to use, the pSi wafers were oxidized for 2 h at 800 °C in a LABEC tube furnace (Laboratory Equipment, Pty. Ltd.).

Preparation of HPG-Grafted pSi. Freshly etched pSi samples were thermally oxidized at 800 °C for 2 h to build a reinforcing oxide layer over the porous structure. This was done to prevent rapid degradation of the pores upon introduction into strong basic solutions. Following thermal oxidation, treatment with RCA at 70 °C for 30 min was used to introduce silanol groups onto the sample surface.[37] Samples were washed with water and ethanol and dried under N_2. Sodium methoxide (0.15 M, 10 mL) was added to the samples under N_2 at 70 °C and reacted for 1 h. Sodium methoxide was removed, and the samples were washed thoroughly with methanol (anhydrous, 3 × 20 mL) and toluene (anhydrous, 3 × 30 mL) using a syringe. Samples were then dried under vacuum at 100 °C for 20 min. Glycidol (distilled the day before and dried over molecular sieves for 18 h) and 1,4-dioxane was added to cover the samples, and polymerization proceeded for 180 min at 100 °C. 1,4-Dioxane was mixed with glycidol in a 1:1 ratio to reduce viscosity and facilitate monomer ingress into the pores. After 180 min at 100 °C under N_2, the unreacted monomer was removed and water was added. The resulting HPG-grafted substrates were washed thoroughly with water and ethanol and dried under N_2.

Preparation of APTES-Functionalized pSi. Thermally oxidized pSi (800 °C for 2 h) was treated with RCA at 70 °C for 30 min to introduce silanol groups onto the surface. The samples were washed with water and ethanol and dried under N_2 and then placed in a solution of (3-aminopropyl)triethoxysilane (APTES) (5% by volume in dry toluene) for 15 min with gentle mixing at room temperature. Unreacted APTES was removed by washing with toluene, and the samples were dried under a stream of N_2.

Preparation of PEG-Grafted Glass Substrates. Glass microscope slides were cleaned by rinsing in 70% ethanol and Milli-Q water then treated with Piranha solution (40% H_2SO_4 and 60% H_2O_2) for 1 h at room temperature. The slides were thoroughly washed with Milli-Q water, dried with compressed air, and dip-coated into a solution of (3-glycidyloxypropyl)trimethoxysilane (GOPTMS) (10% in dry toluene) for 30 min at room temperature. Silanized slides were

thoroughly washed with dry toluene and dried under a stream of N_2. Surface passivation of the silanized slides was carried out under optimized cloud-point conditions using 3000 MW poly(ethylene glycol) bis(amine) (A-PEG).[35] The slides were submerged in a solution of A-PEG (10 mg/mL in 0.1 M phosphate buffer at pH 6.5 containing 0.75 M K_2SO_4) for 24 h at 37 °C.

Protein Resistance Studies. BSA and collagen type I were prepared at concentrations of 100 μg/mL in PBS (pH 7.4). HPG-grafted glass, silicon (prepared via 90 min of glycidol polymerization), and pSi substrates (prepared via 180 min of glycidol polymerization), along with their respective bare substrates, were incubated in the stock protein solutions for 1 h at room temperature in the dark. Subsequently, the samples were washed with PBS, three times for 10 s each time, and Milli-Q, water three times for 10 s each time, and dried under a stream of N_2. XPS was used to analyze the surfaces to compare the nitrogen content introduced by adsorbed proteins.

Cell Attachment Studies. 3T3 fibroblast and T98G glioblastoma cells were maintained in DMEM supplemented with 10% FBS, 100 U/mL penicillin, and 100 μg/mL streptomycin at 37 °C in a humidified atmosphere containing 5% CO_2. The cells were stained separately with 10 μM CellTracker Orange CMRA for 45 min at 37 °C under 5% CO_2. Cells were dissociated from the culture flasks with 0.05% trypsin-0.53 mM EDTA and resuspended in DMEM containing 10% FBS. After centrifugation at 150*g* for 3 min, the cell pellet was resuspended in DMEM containing 10% of FBS. Cells were plated on the HPG-grafted substrates at a density of 5×10^5 cells/cm^2 and then incubated for 4 or 24 h. Unbound cells were removed by gentle washing with sterile PBS. The remaining cells were fixed in 4% paraformaldehyde solution for 30 min and then washed with PBS for 3 min. The immunofluorescence for CellTracker Orange was detected with an inverted fluorescence microscope (Nikon, Eclipse, Ti–S) equipped with the appropriate filter cubes.

RESULTS AND DISCUSSION

Throughout this paper, the terminology used for HPG coated substrates will be abbreviated as follows: Substrate-$HPG_{polymerization\ time\ (minutes)}$. For example, HPG polymerized on glass slide for 90 min is shortened to G-HPG_{90}, and HPG polymerized on porous silicon for 180 min is shortened to pSi-HPG_{180}.

Surface-Initiated HPG Growth. Surface-initiated, anionic ring opening polymerization of glycidol was carried out on glass, flat silicon, and pSi substrates. The flat substrates were initially treated with RCA cleaning solution to remove organic residues and convert exposed silicon oxide to silicon hydroxide (silanol) groups.[38] Sodium methoxide solution was then employed to activate the surface of the substrate by deprotonation of the silanol groups. To avoid bulk polymerization upon addition of the monomer, excess sodium methoxide solution was removed, and the surfaces were thoroughly washed with anhydrous methanol and toluene. Glycidol was added under nitrogen and polymerized for 90 min at 100 °C from the activated surfaces to yield uniform high-density polymer brushes. The proposed mechanism for surface-initiated polymerization of glycidol to afford grafted HPGs (Scheme 1)[32] is similar to that proposed for bulk polymerization.[39] Therefore, polymerization times of 20, 40, 60, and 90 min were studied from silicon substrates to investigate the time-dependent increase in polymer content on the surface.

HPG was also grafted from the porous substrate pSi. Here, a slightly modified approach was used: Freshly etched pSi samples were thermally oxidized at 800 °C for 2 h, after which time, the temperature was slowly decreased to room temperature overnight. Thermal oxidation creates a silica layer over the pSi structure, helping increase structural integrity and stability when the sample is exposed to strong basic solutions.[40] Following thermal oxidation, the samples appeared to have lost some of the color indicative of porous silicon, and the etched layer had become slightly transparent. This was due to the formation of a glassy silica layer during oxidation.[41] However, SEM analysis of the surface confirmed the presence of pores post oxidation. SEM images taken across the porous surface showed an average pore size of 16 ± 3 nm in diameter (Figure 1). Following thermal oxidation of the porous structures, RCA

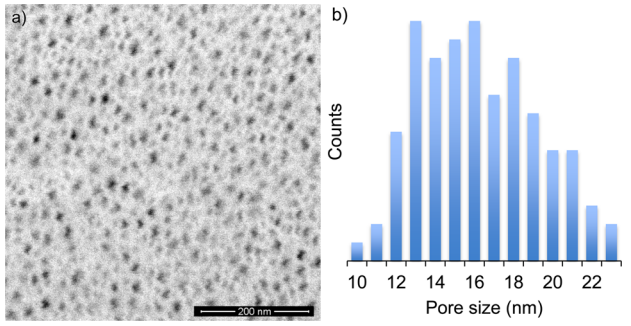

Figure 1. (a) Representative SEM image of thermally oxidized pSi, scale bar = 200 nm. (b) Pore diameters accumulated from 100 measurements across three images.

cleaning and surface activation with sodium methoxide proceeded the same as for the flat substrates. However, HPG growth from pSi differed slightly from flat substrates in that 1,4-dioxane was added as a solvent to reduce the viscosity of glycidol during polymerization and aid monomer penetration into the pores. Glycidol was diluted by 50% when polymerizing from pSi; therefore, polymerization time was doubled to 180 min to compensate for the reduced monomer concentration.

Surface Analysis. XPS analysis of the HPG-grafted glass, flat silicon, and pSi substrates confirmed the presence of HPG on the surface based on the appearance of a characteristic etheric carbon peak at ∼286.6 eV in the high-resolution C 1s spectrum (Figure 2).[42]

The carbon content for Si-HPG_{20-90} increased linearly with respect to polymerization time, while the silicon content decreased at the same rate (Figure 2d). From this linear trend, we infer consistent HPG growth from initiation through 90 min of polymerization. The continued presence of silicon in the XPS spectra indicates that very thin coatings (<10 nm) had been produced even after 90 min of polymerization, given that the information depth for XPS is generally limited to the outer 10 nm. With the assumption that the HPG coatings were pinhole free, approximate graft thicknesses were calculated from the attenuation of the silicon concentration in the XPS spectra. HPG-graft thicknesses were calculated to be ∼4.6, ∼2.4, and ∼2.9 nm for Si-HPG_{90}, G-HPG_{90}, and pSi-HPG_{180}, respectively.

An alternative explanation for the silicon content after HPG grafting could be that there are pinholes or voids in the coating. Therefore, atomic force microscopy (AFM) was employed to determine the roughness of the HPG-grafted surfaces. Roughness was measured first in the dry state and then in the hydrated state by placing a drop of Milli-Q water over the cantilever (Table 1). Si-HPG_{90} in the dry and hydrated states had an RMS roughness (Rq) of 0.6 and 0.7 nm, respectively. The Rq of polished silicon wafers was 0.2 nm, which is in agreement with the literature, while the Rq for RCA treated silicon wafers was much higher at 0.9 nm.[43] The increase in

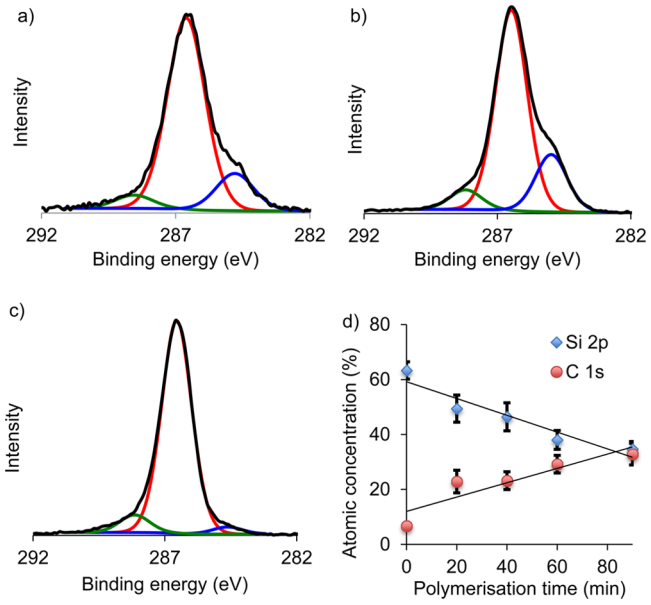

Figure 2. High-resolution C 1s XPS spectra obtained after the polymerization of glycidol initiated from (a) silicon wafer, (b) glass microscope slide, and (c) pSi at 100 °C for 90 min. (d) Evolution of carbon and silicon content for Si-HPG$_{20-90}$ derived from XPS survey data. The dominant etheric carbon peak at 286.6 eV (red line) indicates the presence of HPGs on the surface. Peaks at 285.0 eV (blue line, C−C) and 288.5 eV (green line, C═O) were attributed to adventitious carbon.

roughness of the silicon wafer following RCA treatment was attributed to etching of the surface caused by the RCA over a 30 min clean.[44] Therefore, Si-HPG$_{90}$ in the dry and hydrated states exhibited very flat surfaces free of voids or pinholes, indicating that HPG growth was dense and uniform across the surface. G-HPG$_{90}$ had an Rq of 0.7 nm in the dry state and 0.7 nm in the hydrated state. Measured Rq values for bare glass and RCA treated glass substrates were 0.5 and 1.2 nm, respectively. The large increase in roughness following RCA treatment was once again due to the roughening of the surface during the RCA etch. Similar to HPG-grafted silicon, low roughness values for G-HPG$_{90}$ and the absence of voids or pinholes indicate homogeneous distribution of the grafted HPG over the substrate. The slight increase in roughness in the hydrated state for both HPG-grafted silicon and glass was attributed to swelling of the globular HPG structures, exacerbating undulations caused by the globular structures. Under the solvation conditions studied previously for the grafting-to approach, limitations in grafting densities leave well-defined globular structures across the surface, resulting in much higher surface roughness with Rq values between 1.05 and 1.17 nm.[25] In contrast, the polymerization of glycidol from surface-bound initiators appears to permit high grafting densities such that individual molecules can no longer be resolved via this technique and therefore produces surfaces with reduced roughness in both the dehydrated and hydrated states.

Ellipsometry measurements of Si-HPG$_{90}$ and G-HPG$_{90}$ samples revealed a dehydrated polymer brush thicknesses of 3.2 ± 0.1 nm and 2.6 ± 0.8 nm, respectively. Measured thicknesses are in agreement with XPS results.

Sessile drop water contact angle measurements were also recorded for the HPG-grafted surfaces because they afford insights into the wettability (Table 1). An initial contact angle of 47 ± 2° for silicon with a thin native oxide layer was in agreement with the literature.[45] After 20 min of glycidol polymerization, the contact angle remained within the range of statistical error of the bare silicon substrate (Table 1), indicating that HPG grafting density and film thickness at this time were low. A significant increase in wettability was observed for Si-HPG$_{40}$ with a contact angle of 39 ± 3°, which was attributed to an increase in hydroxyl groups at the surface. Wettability continued to increase as polymerization was permitted to proceed for up to 90 min. This was attributed to the continued increase in hydroxyl functionality at the surface as HPG grafting density and film thickness increased over time.

In contrast to the silicon substrates, the glass substrates were highly hydrophilic with a contact angle of 17 ± 1° (Table 1). Following 90 min of polymerization with glycidol, the contact angle was observed to increase to 28 ± 1°, similar to the contact angle of Si-HPG$_{90}$. Although glass substrates exhibited the opposite trend to silicon substrates, the change in wettability indicates a change in surface chemistry. This, along with the appearance of etheric carbon in the XPS spectrum, confirms the successful grafting of HPG from glass substrates.

Silane-modified HPGs with MWs of 2000 g/mol grafted to glass substrates have been reported to display contact angles of 21 ± 1°, while thiol-modified 2500 and 5000 g/mol HPGs grafted to gold substrates had contact angles of 20 ± 2° and 20 ± 3°, respectively.[22,24] Therefore, the grafting-from approach appears to produce surfaces that are slightly more hydrophilic

Table 1. Summary of Surface Analytical Data Obtained on HPG-Grafted Glass, Flat Silicon, and pSi Substrates

sample	C atomic concn (%)[a]	Si atomic concn (%)[a]	O atomic concn (%)[a]	% C−O/C[b]	contact angle (deg)	thickness (nm)[c]	roughness, Rq (nm)[d]
silicon	3.2	64.3	32.5		47 ± 2		0.1
Si-HPG$_{20}$	22.9	49.4	27.3	55.7	50 ± 1		
Si-HPG$_{40}$	23.2	46.4	29.9	79.1	39 ± 3		
Si-HPG$_{60}$	29.2	38.0	32.8	79.3	32 ± 2		
Si-HPG$_{90}$	32.8	34.6	31.9	85.0	23 ± 1	3.2 ± 0.1	0.6
glass	14.4	29.4	51.2		17 ± 1		0.5
G-HPG$_{90}$	25.5	22.5	46.4	71.1	28 ± 1	2.6 ± 0.8	0.7
pSi-Ox	1.4	40.1	58.5				
pSi-HPG$_{180}$	20.9	28.3	50.8				
G-PEG	44.2	17.1	37.1				

[a]Elemental composition from XPS survey spectra. [b]Contribution of etheric carbon content within the deconvoluted high-resolution XPS C 1s spectra. [c]Determined via ellipsometry in the dehydrated state. [d]Determined by AFM in the dehydrated state.

in nature. These small differences can be attributed to differences in surface roughness, which affect the contact angle according to the Wenzel model.[46]

Protein Resistance of HPG-Grafted Surfaces. The adhesion of proteins to a surface is the first step in biofouling and provides a mechanism for cell attachment. For a surface to be resistant to cell attachment, it must first be resistant to protein adsorption. Factors that contribute to the attraction and repulsion of proteins from polymer films include hydrophobic or charge interactions, temperature, pH, and interfacial free energies between the polymer and water.[13,15,47] However, HPGs are hydrophilic and neutral, so the contributing factor toward protein repulsion is the steric barrier caused by the high conformational entropy of HPG-grafted surfaces.[14,48−52] We examined the effectiveness of G-HPG$_{90}$, Si-HPG$_{90}$, and pSi-HPG$_{180}$ to repel proteins of two different molecular weights and compared these to uncoated surfaces: Bovine serum albumin (BSA) is a relatively small protein with a molecular weight (MW) of 66.5 kDa commonly used as a nutrient in cell and tissue culture. Collagen type I is the most abundant protein in mammals and is a much larger protein than BSA at ∼400 kDa for the trimeric form.[53] G-HPG$_{90}$, Si-HPG$_{90}$, and pSi-HPG$_{180}$, along with their bare controls, were incubated in PBS (pH 7.4) solutions of these biomolecules individually at 100 μg/mL for 1 h at room temperature.[54] XPS was used to analyze the surfaces and quantify the nitrogen content. Note that there is no nitrogen in either the bare or HPG-grafted substrates prior to adsorption studies. Therefore, the introduction of significant levels of nitrogen indicates adsorbed protein on the surface (Figure 3).

All three HPG-grafted substrates exhibited greatly reduced nitrogen signatures compared to their uncoated counterparts following incubation with the two proteins. This indicated that the grafted HPG provided a high level of resistance to adhesion of the two proteins studied.

The adsorption of BSA was reduced by 73, 88, and 97% on G-HPG$_{90}$, Si-HPG$_{90}$, and pSi-HPG$_{180}$, respectively. These values are consistent with studies conducted on HPG-grafted substrates prepared via grafting-to approaches: Self-assembled monolayers (SAMs) of single thiol modified HPGs on gold reduced BSA adhesion by up to 75%, while PEG SAMs prepared the same way reduced BSA adhesion by only 62%.[25] Similarly, monolayers of silane-modified HPGs reduced BSA adhesion by up to 96%, while silane-modified PEG monolayers achieved 89% reduction.[24]

For collagen type I, the reduction of protein adsorption was just as efficient with 84, 91, and 83% for G-HPG$_{90}$, Si-HPG$_{90}$, and pSi-HPG$_{180}$, respectively. The efficiencies seen here for the reduction in both BSA and collagen type I adhesion to HPG-grafted substrates indicate that the antifouling properties of the coatings cover a range of biomolecule sizes and types. The low level of protein adsorption seen for the HPG-grafted substrates suggests small defect sites exist across the surfaces, allowing the interaction of a small quantity of proteins with the substrate below. These defects could be in the form of very small pinholes in the HPG layer or areas where the HPG is not thick enough to overcome interactions between the proteins and the solid substrate. Continued optimization of grafting conditions, including graft density and polymerization time, could potentially reduce protein adsorption even further.

It should be noted that the adsorption of proteins onto solid substrates is affected by a range of factors, including charge of the surface and protein, size of the protein, ionic strength, and pH of the solution.[55] Therefore, it is difficult to generalize the results shown here into more complicated systems such as whole blood, which is the focus of ongoing studies.

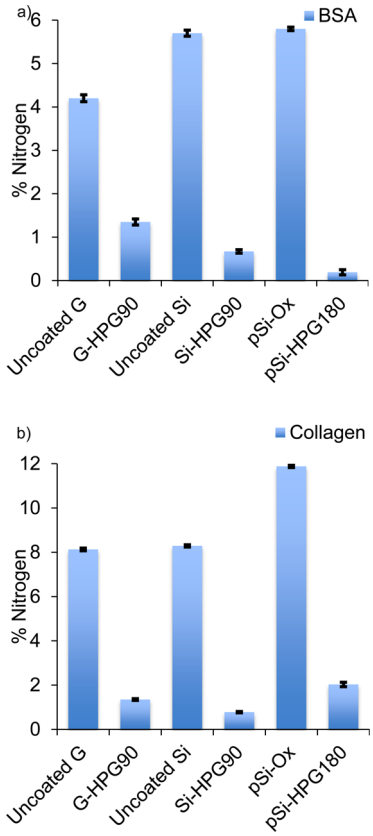

Figure 3. Comparison of the nitrogen atomic concentration, as determined by XPS, between uncoated glass, flat silicon, and thermally oxidized pSi controls and the corresponding HPG-grafted substrates after incubation with (a) BSA and (b) collagen type I at concentrations of 100 μg/mL for 1 h at room temperature.

Resistance of HPG-Grafted Surfaces to Mammalian Cell Attachment. The above results from protein adsorption suggest that HPG-grafted surfaces may also resist cell attachment. To study the resistance of HPG-grafted silicon, glass, and pSi surfaces to cell attachment, we incubated two anchorage-dependent cell lines, T98G human glioblastoma cells, and 3T3 mouse fibroblast cells, separately with the HPG-grafted substrates for 4 and 24 h (Figure 4). A high cell seeding density of 5×10^5 cells/cm^2 was used for both cell lines in order to challenge the surfaces. Controls included uncoated silicon wafer, uncoated glass microscope slide, pSi with uncoated oxide layer (pSi-Ox), and pSi functionalized with APTES (pSi-APTES). Previous studies have demonstrated that the hydrophilic nature of oxidized pSi has prevented the attachment of some cell lines in high density.[37] Therefore, APTES-functionalized pSi was produced as a positive control for cell attachment. However, under the conditions used here, cell densities proved comparable between pSi-Ox and pSi-APTES (Table 2).

Figure 4 shows representative images of Si-HPG$_{90}$, G-HPG$_{90}$, and pSi-HPG$_{180}$, along with uncoated substrates, after 4 and 24 h of incubation with T98G cells in serum-containing medium. After 4 h, a near confluent layer of cells had formed on the uncoated flat substrates with more than 140 000 and 130 000 cells/cm^2 for silicon and glass, respectively, while cell densities

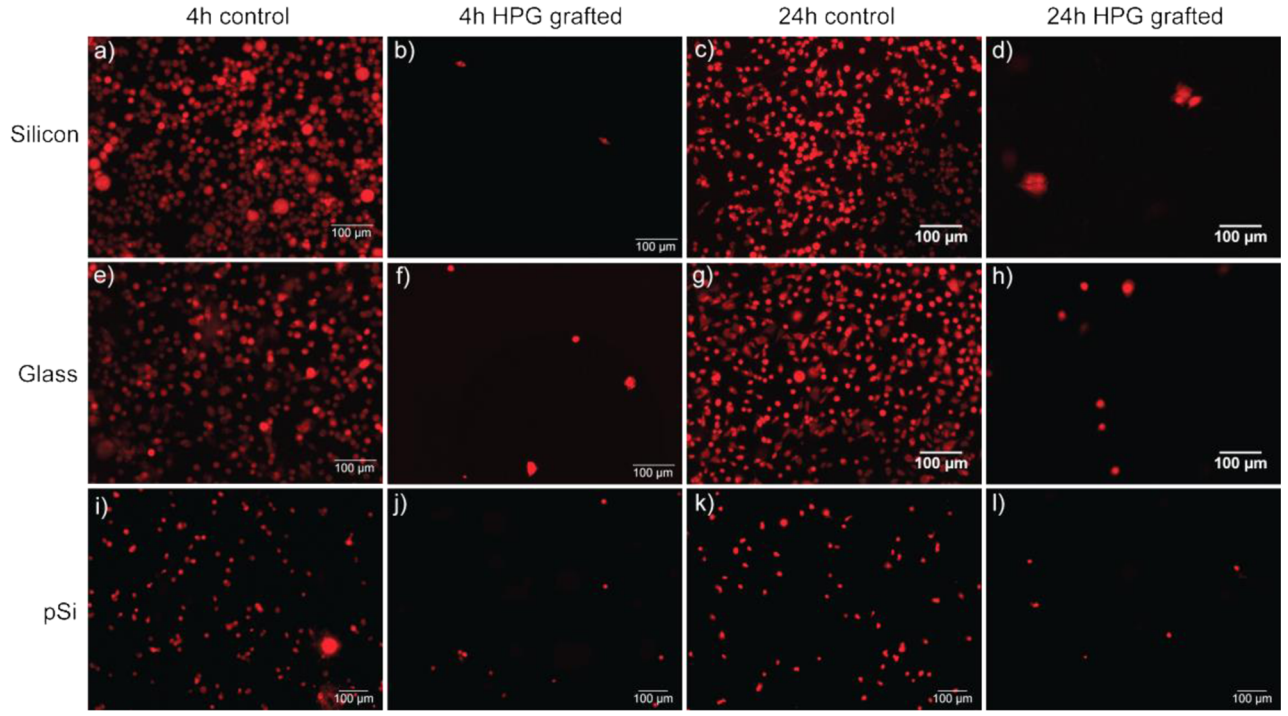

Figure 4. Fluorescence microscopy images of T98G human glioblastoma cells stained with CellTracker Orange incubated on (a) bare silicon wafer for 4 h, (b) Si-HPG_{90} for 4 h, (c) bare silicon wafer for 24 h, (d) Si-HPG_{90} for 24 h, (e) bare glass slide for 4 h, (f) G-HPG_{90} for 4 h, (g) bare glass slide for 24 h, (h) G-HPG_{90} for 24 h, (i) bare pSi-Ox for 4 h, (j) pSi-HPG_{180} for 4 h, (k) bare pSi-Ox for 24 h, and (l) pSi-HPG_{180} for 24 h. Scale bars = 100 μm.

Table 2. T98G Human Glioblastoma and 3T3 Mouse Fibroblast Cell Densities After 4 h and (24 h) of Incubation with Seeding Densities of 5×10^5 cells/cm^2

	T98G cells		3T3 fibroblasts	
sample	cells $\times 10^2$ cm^{-2}	% redn[a]	cells $\times 10^2$ cm^{-2}	% redn[a]
silicon wafer	1,431 ± 20	0	180 ± 18	0
	(1,450 ± 21)	(0)	(130 ± 15)	(0)
glass slide	1,306 ± 22	0	83 ± 12	0
	(1,299 ± 21)	(0)	(86 ± 14)	(0)
pSi-Ox	153 ± 16	0	92 ± 30	0
	(114 ± 25)	(0)	(7 ± 1)	(0)
pSi-APTES	132 ± 29	0	179 ± 14	0
	(98 ± 22)	(0)	(92 ± 37)	(0)
Si-HPG_{90}	5 ± 1	99.6	2 ± 1	98.8
	(13 ± 1)	(99.1)	(1 ± 1)	(99.2)
G-HPG_{90}	14 ± 2	99.0	3 ± 1	96.8
	(16 ± 1)	(98.8)	(2 ± 1)	(97.4)
pSi-HPG_{180}	4 ± 2	97.2	3 ± 1	98.3
	(4 ± 1)	(96.1)	(1 ± 1)	(98.8)
G-PEG[b]	116 ± 11	91.1	5 ± 2	94.3
	(37 ± 6)	(97.2)	(130 ± 27)	(0)

[a]Percent reduction in cell attachment with respect to silicon wafer, glass, or pSi-APTES. [b]Fibroblast attachment to monolayers of G-PEG.

on both pSi controls were considerably lower at ~15 000 cells/cm^2 (Table 2). In comparison, Si-HPG_{90}, G-HPG_{90} and pSi-HPG_{180} exhibited very low levels of cell attachment, and T98G cell attachment was reduced by 99.6, 99.0, and 97.2%, respectively. After 24 h of incubation, cell densities remained relatively constant across the control substrates with respect to 4 h of incubation (Table 2).

Cell attachment on Si-HPG_{90} had doubled after 24 h of incubation in comparison to 4 h of incubation. However, this was generally due to the appearance of clusters of cells and not an increase in individual cells across the surface, most likely caused by proliferation of the attached cells (Figure 4c). Reduction in cell attachment compared to the bare silicon wafer still remained greater than 99% (Table 2). G-HPG_{90} and pSi-HPG_{180} showed no increase in cell density from 4 to 24 h. The few cells attached to the HPG-grafted substrates had begun to spread after 24 h of incubation, which indicates that they had been able to find extracellular matrix proteins adsorbed on the surface. All three HPG-grafted substrates demonstrated increased resistance to T98G cell attachment as compared to PEG-grafted glass (G-PEG) with comparable film thickness.[35] PEG coatings produced with 3000 g/mol chains under optimized cloud-point grafting conditions still contained ~17% silicon in the XPS spectrum, similar to G-HPG_{90}, indicating coatings were less than 10 nm thick (Table 1). Reduction in T98G cell attachment after 4 h was 91.1%, significantly less effective than for HPG-grafted substrates. However, following 24 h of incubation, cell density on G-PEG had reduced to approximately one-third of the cells attached after 4 h, bringing the reduction in cell attachment of G-PEG up to 97.2%. The reduction in cell attachment after 24 h, with respect to 4 h, suggests that loosely attached cells lifted off after a longer incubation period. However, HPG-grafted substrates all exhibited antifouling properties as good as or better than G-PEG for T98G cells.

The antifouling properties of HPG-grafted substrates were also tested on 3T3 fibroblasts, which are another anchorage-dependent cell line that are highly adherent to a broad range of surfaces.[56] Fibroblast cells were incubated with a cell seeding density of 5×10^5 cells/cm^2 on Si-HPG_{90}, G-HPG_{90}, and pSi-

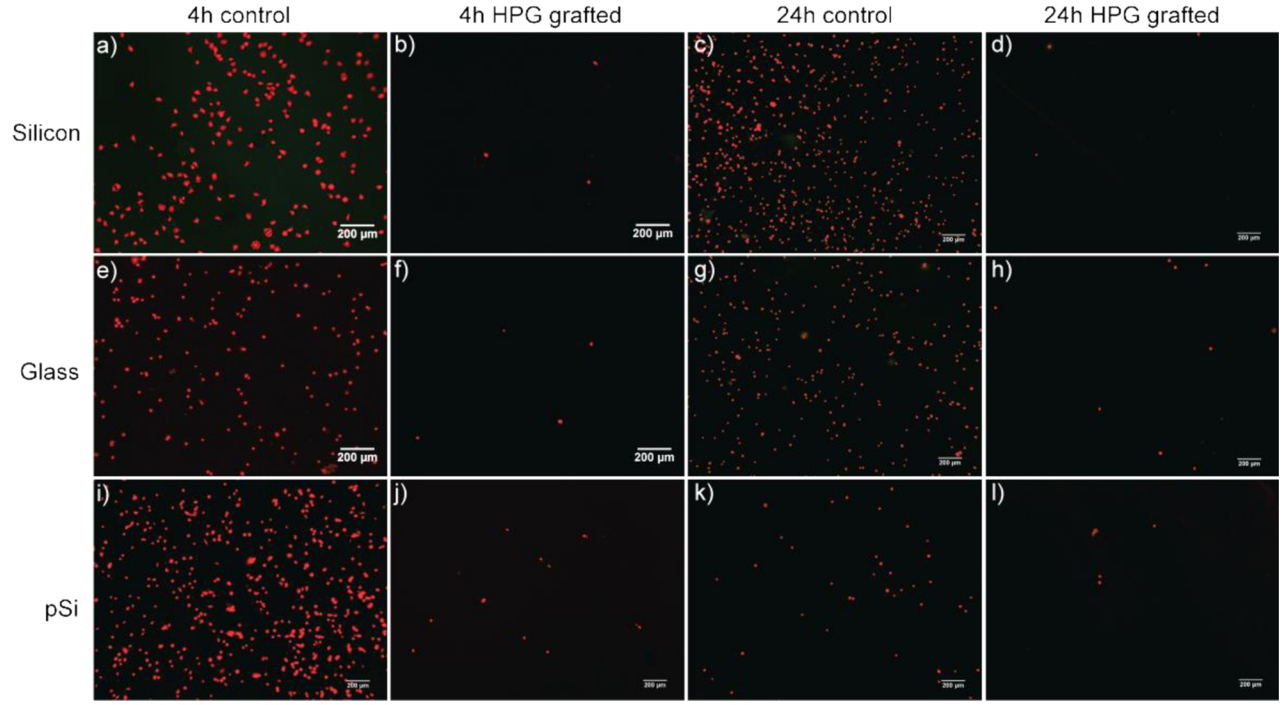

Figure 5. Fluorescence microscopy images of 3T3 fibroblast cells stained with CellTracker Orange incubated on (a) bare silicon wafer for 4 h, (b) Si-HPG_{90} for 4 h, (c) bare silicon wafer for 24 h, (d) Si-HPG_{90} for 24 h, (e) bare glass slide for 4 h, (f) G-HPG_{90} for 4 h, (g) bare glass slide for 24 h, (h) G-HPG_{90} for 24 h, (i) bare pSi-Ox for 4 h, (j) pSi-HPG for 4 h, (k) bare pSi-Ox for 24 h, and (l) pSi-HPG for 24 h. Scale bars = 200 μm.

HPG_{180}, along with their respective uncoated substrates, for 4 and 24 h (Figure 5). Even though the cell seeding density for the sticky fibroblasts was the same as for the T98G cells, cell densities on the control substrates after 4 and 24 h were much lower than those seen for the T98G cells. However, fibroblast cell numbers on Si-HPG_{90}, G-HPG_{90}, and pSi-HPG_{180} after 24 h incubation were still reduced by 99.2, 97.4, and 98.8%, respectively, compared to the control substrates (Table 2).

The two cell types studied here were chosen for their renowned adherence in order to challenge the HPG-grafted substrates. While a significant reduction in T98G and 3T3 cell attachment was observed here, one should not deduce from these findings that these substrates behave the same for all cell types. However, this is a good basis for further investigations to find the limitations of this system.

Fibroblast cell densities for Si-HPG_{90}, G-HPG_{90}, and pSi-HPG_{180} were considerably lower than for G-PEG after both 4 and 24 h incubation (Table 2). After just 4 h of incubation, the PEG-grafted substrate exhibited relatively high resistance to fibroblast cell attachment with a reduction of 94.3% compared to that of the uncoated substrate. However, after 24 h of incubation, G-PEG exhibited greater fibroblast cell attachment than the uncoated substrate with 13 000 and 8600 cells/cm^2, respectively. Therefore, the HPG-grafted substrates exhibited superior resistance to attachment from both T98G cells and fibroblast cells over a 24 h period. Even though the G-PEG samples were all prepared under cloud-point conditions at the same time, these surfaces were overcome by fibroblast attachment after 24 h of incubation. This indicates the antifouling properties of these substrates cannot be generalized across all cell types and that further optimizations would be needed to provide long-term reduction in attachment of some cell types. More sophisticated PEG architectures such as star-PEG hydrogels and surface-initiated PEG brushes have been shown to produce very effective low-fouling surfaces.[16−18] These alternative PEG architectures could potentially show improved resistance to cell attachment over the linear PEG studied here. However, these systems are not currently used routinely in commercial applications, as linear PEG is, and were therefore not studied here as comparators for HPGs.

CONCLUSIONS

Here, we demonstrate the ultralow-fouling properties of HPG-grafted silicon, pSi, and glass substrates. Glycidol was polymerized from deprotonated silanol functional groups on glass, silicon, and porous silicon substrates. A polymerization time of 90 min produced thin HPG films of approximately 3 nm thickness for both flat silicon and glass substrates. These thin films showed high resistance to protein adsorption of both BSA and collagen type I from solution. Human glioblastoma and mouse fibroblast cell attachment on the HPG coatings was reduced by as much as 99.6% compared to that of uncoated substrates. The ultralow-fouling properties of HPG coatings produced by the grafting-from approach performed as well as if not better than PEG coatings of similar thickness produced by an optimized grafting-to approach. HPG coatings produced here via the grafting-from approach provide several key benefits over PEG coatings, such as increased stability against oxidation and increased chemical functionality at the surface of the coating. Furthermore, due to the time-dependent growth of the HPG film, the thickness and density of these coatings can be tailored and optimized to overcome challenges provided under different experimental conditions. Therefore, HPG coatings would be ideal candidates for use in a broad range of biomedical applications where robust antifouling properties are required. Not only could HPG graft polymer coatings replace PEG coatings in several existing applications, but HPG could also fill new roles where both antifouling and highly functional

films are required. For example, antifouling substrates in lab-on-a-chip microarrays where the substrate needs to exhibit ultralow-fouling properties while providing suitable bioconjugate chemistries.[57−59]

■ ASSOCIATED CONTENT

Supporting Information

AFM cross sections of bare silicon wafer, bare glass microscope slide, and respective HPG-grafted substrates. This material is available free of charge via the Internet at http://pubs.acs.org.

■ AUTHOR INFORMATION

Corresponding Author

*E-mail: nico.voelcker@unisa.edu.au.

Notes

The authors declare no competing financial interest.

■ REFERENCES

(1) Senaratne, W.; Andruzzi, L.; Ober, C. K. Self-Assembled Monolayers and Polymer Brushes in Biotechnology: Current Applications and Future Perspectives. *Biomacromolecules* **2005**, *6*, 2427−2448.

(2) Banerjee, I.; Pangule, R. C.; Kane, R. S. Antifouling Coatings: Recent Developments in the Design of Surfaces That Prevent Fouling by Proteins, Bacteria, and Marine Organisms. *Adv. Mater.* **2011**, *23*, 690−718.

(3) Cole, N.; Hume, E. B. H.; Vijay, A. K.; Sankaridurg, P.; Kumar, N.; Willcox, M. D. P. In Vivo Performance of Melimine as an Antimicrobial Coating for Contact Lenses in Models of CLARE and CLPU. *Invest. Ophthalmol. Visual Sci.* **2010**, *51*, 390−395.

(4) Ohko, Y.; Utsumi, Y.; Niwa, C.; Tatsuma, T.; Kobayakawa, K.; Satoh, Y.; Kubota, Y.; Fujishima, A. Self-Sterilizing and Self-Cleaning of Silicone Catheters Coated with TiO_2 Photocatalyst Thin Films: A Preclinical Work. *J. Biomed. Mater. Res., Part A* **2001**, *58*, 97−101.

(5) Vasilev, K.; Cook, J.; Griesser, H. J. Antibacterial Surfaces for Biomedical Devices. *Expert Rev. Med. Devices* **2009**, *6*, 553−567.

(6) Willcox, M. D. P.; Hume, E. B. H.; Aliwarga, Y.; Kumar, N.; Cole, N. A Novel Cationic-Peptide Coating for the Prevention of Microbial Colonization on Contact Lenses. *J. Appl. Microbiol.* **2008**, *105*, 1817−1825.

(7) Hucknall, A.; Rangarajan, S.; Chilkoti, A. In Pursuit of Zero: Polymer Brushes That Resist the Adsorption of Proteins. *Adv. Mater.* **2009**, *21*, 2441−2446.

(8) Thissen, H.; Gengenbach, T.; du Toit, R.; Sweeney, D. F.; Kingshott, P.; Griesser, H. J.; Meagher, L. Clinical Observations of Biofouling on PEO Coated Silicone Hydrogel Contact Lenses. *Biomaterials* **2010**, *31*, 5510−5519.

(9) Page, K.; Wilson, M.; Parkin, I. P. Antimicrobial Surfaces and Their Potential in Reducing the Role of the Inanimate Environment in the Incidence of Hospital-Acquired Infections. *J. Mater. Chem.* **2009**, *19*, 3819−3831.

(10) Amiji, M.; Park, K. Surface Modification of Polymeric Biomaterials with Poly(ethylene oxide), Albumin, and Heparin for Reduced Thrombogenicity. *J. Biomater. Sci., Polym. Ed.* **1993**, *4*, 217−234.

(11) Liu, V. A.; Jastromb, W. E.; Bhatia, S. N. Engineering Protein and Cell Adhesivity Using PEO-Terminated Triblock Polymers. *J. Biomed. Mater. Res., Part A* **2002**, *60*, 126−134.

(12) Kingshott, P.; Thissen, H.; Griesser, H. J. Effects of Cloud-Point Grafting, Chain Length, and Density of Peg Layers on Competitive Adsorption of Ocular Proteins. *Biomaterials* **2002**, *23*, 2043−2056.

(13) Zdyrko, B.; Varshney, S. K.; Luzinov, I. Effect of Molecular Weight on Synthesis and Surface Morphology of High-Density Poly(ethylene glycol) Grafted Layers. *Langmuir* **2004**, *20*, 6727−6735.

(14) McNamee, C. E.; Yamamoto, S.; Higashitani, K. Effect of the Physicochemical Properties of Poly(ethylene glycol) Brushes on Their Binding to Cells. *Biophys. J.* **2007**, *93*, 324−334.

(15) Unsworth, L. D.; Sheardown, H.; Brash, J. L. Polyethylene Oxide Surfaces of Variable Chain Density by Chemisorption of PEO-Thiol on Gold: Adsorption of Proteins from Plasma Studied by Radiolabelling and Immunoblotting. *Biomaterials* **2005**, *26*, 5927−5933.

(16) Liu, S. Q.; Yang, C.; Huang, Y.; Ding, X.; Li, Y.; Fan, W. M.; Hedrick, J. L.; Yang, Y.-Y. Antimicrobial and Antifouling Hydrogels Formed in Situ from Polycarbonate and Poly(ethylene glycol) via Michael Addition. *Adv. Mater.* **2012**, *24*, 6484−6489.

(17) Kizhakkedathu, J. N.; Janzen, J.; Le, Y.; Kainthan, R. K.; Brooks, D. E. Poly(oligo(ethylene glycol)acrylamide) Brushes by Surface Initiated Polymerization: Effect of Macromonomer Chain Length on Brush Growth and Protein Adsorption from Blood Plasma. *Langmuir* **2009**, *25*, 3794−3801.

(18) Ma, H.; Hyun, J.; Stiller, P.; Chilkoti, A. "Non-Fouling" Oligo(ethylene glycol)-Functionalized Polymer Brushes Synthesized by Surface-Initiated Atom Transfer Radical Polymerization. *Adv. Mater.* **2004**, *16*, 338−341.

(19) Moore, E.; Thissen, H.; Voelcker, N. H. Hyperbranched Polyglycerols at the Biointerface. *Prog. Surf. Sci.* **2013**, *88*, 213−236.

(20) Haag, R.; Stumbe, J.-F.; Sunder, A.; Frey, H.; Hebel, A. An Approach to Core-Shell-Type Architectures in Hyperbranched Polyglycerols by Selective Chemical Differentiation. *Macromolecules* **2000**, *33*, 8158−8166.

(21) Shen, Y.; Kuang, M.; Shen, Z.; Nieberle, J.; Duan, H.; Frey, H. Gold Nanoparticles Coated with a Thermosensitive Hyperbranched Polyelectrolyte: Towards Smart Temperature and pH Nanosensors. *Angew. Chem., Int. Ed.* **2008**, *47*, 2227−2230.

(22) Siegers, C.; Biesalski, M.; Haag, R. Self-Assembled Monolayers of Dendritic Polyglycerol Derivatives on Gold That Resist the Adsorption of Proteins. *Chem.—Eur. J.* **2004**, *10*, 2831−8.

(23) Deschamps, A. A.; Grijpma, D. W.; Feijen, J. Poly(ethylene oxide)/Poly(butylene terephthalate) Segmented Block Copolymers: The Effect of Copolymer Composition on Physical Properties and Degradation Behavior. *Polymer* **2001**, *42*, 9335−9345.

(24) Weinhart, M.; Becherer, T.; Schnurbusch, N.; Schwibbert, K.; Kunte, H.-J.; Haag, R. Linear and Hyperbranched Polyglycerol Derivatives as Excellent Bioinert Glass Coating Materials. *Adv. Eng. Mater.* **2011**, B501−B510.

(25) Kainthan, R. K.; Zou, Y.; Chiao, M.; Kizhakkedathu, J. N. Self-Assembled Monothiol-Terminated Hyperbranched Polyglycerols on a Gold Surface: A Comparative Study on the Structure, Morphology, and Protein Adsorption Characteristics with Linear Poly(ethylene glycol)s. *Langmuir* **2008**, *24*, 4907−4916.

(26) Wyszogrodzka, M.; Haag, R. Study of Single Protein Adsorption onto Monoamino Oligoglycerol Derivatives: A Structure-Activity Relationship. *Langmuir* **2009**, *25*, 5703−5712.

(27) Wyszogrodzka, M.; Haag, R. Synthesis and Characterization of Glycerol Dendrons, Self-Assembled Monolayers on Gold: A Detailed Study of Their Protein Resistance. *Biomacromolecules* **2009**, *10*, 1043−1054.

(28) Kopf, A.; Baschnagel, J.; Wittmer, J.; Binder, K. On the Adsorption Process in Polymer Brushes: A Monte Carlo Study. *Macromolecules* **1996**, *29*, 1433−1441.

(29) Jeon, H.; Schmidt, R.; Barton, J. E.; Hwang, D. J.; Gamble, L. J.; Castner, D. G.; Grigoropoulos, C. P.; Healy, K. E. Chemical Patterning of Ultrathin Polymer Films by Direct-Write Multiphoton Lithography. *J. Am. Chem. Soc.* **2011**, *133*, 6138−6141.

(30) Bose, R. K.; Nejati, S.; Stufflet, D. R.; Lau, K. K. S. Graft Polymerization of Anti-Fouling PEO Surfaces by Liquid-Free Initiated Chemical Vapor Deposition. *Macromolecules* **2012**, *45*, 6915−6922.

(31) Fan, X.; Lin, L.; Messersmith, P. B. Cell Fouling Resistance of Polymer Brushes Grafted from Ti Substrates by Surface-Initiated Polymerization: Effect of Ethylene Glycol Side Chain Length. *Biomacromolecules* **2006**, *7*, 2443−2448.

(32) Khan, M.; Huck, W. T. S. Hyperbranched Polyglycidol on Si/SiO_2 Surfaces Via Surface-Initiated Polymerization. *Macromolecules* **2003**, *36*, 5088−5093.

(33) Flavel, B. S.; Sweetman, M. J.; Shearer, C. J.; Shapter, J. G.; Voelcker, N. H. Micropatterned Arrays of Porous Silicon: Toward Sensory Biointerfaces. *ACS Appl. Mater. Interfaces* **2011**, *3*, 2463−2471.
(34) Vasani, R. B.; McInnes, S. J. P.; Cole, M. A.; Jani, A. M. M.; Ellis, A. V.; Voelcker, N. H. Stimulus-Responsiveness and Drug Release from Porous Silicon Films ATRP-Grafted with Poly(*N*-isopropylacrylamide). *Langmuir* **2011**, *27*, 7843−7853.
(35) Rasi Ghaemi, S.; Harding, F.; Delalat, B.; Vasani, R.; Voelcker, N. H. Surface Engineering for Long-Term Culturing of Mesenchymal Stem Cell Microarrays. *Biomacromolecules* **2013**, *14*, 2675−2683.
(36) Pace, S.; Vasani, R. B.; Cunin, F.; Voelcker, N. H. Study of the Optical Properties of a Thermoresponsive Polymer Grafted onto Porous Silicon Scaffolds. *New J. Chem.* **2013**, *37*, 228−235.
(37) Low, S. P.; Williams, K. A.; Canham, L. T.; Voelcker, N. H. Evaluation of Mammalian Cell Adhesion on Surface-Modified Porous Silicon. *Biomaterials* **2006**, *27*, 4538−46.
(38) Lickiss, P. D. The Synthesis and Structure of Organosilanols. *Adv. Inorg. Chem.* **1995**, *42*, 147−262.
(39) Sunder, A.; Hanselmann, R.; Frey, H.; Mulhaupt, R. Controlled Synthesis of Hyperbranched Polyglycerols by Ring-Opening Multibranching Polymerization. *Macromolecules* **1999**, *32*, 4240−4246.
(40) Jarvis, K. L.; Barnes, T. J.; Prestidge, C. A. Surface Chemistry of Porous Silicon and Implications for Drug Encapsulation and Delivery Applications. *Adv. Colloid Interface Sci.* **2012**, *175*, 25−38.
(41) Nakamura, T.; Ogawa, T.; Hosoya, N.; Adachi, S. Effects of Thermal Oxidation on the Photoluminescence Properties of Porous Silicon. *J. Lumin.* **2010**, *130*, 682−687.
(42) Sharma, S.; Johnson, R. W.; Desai, T. A. XPS and AFM Analysis of Antifouling PEG Interfaces for Microfabricated Silicon Biosensors. *Biosens. Bioelectron.* **2004**, *20*, 227−239.
(43) Krzywiecki, M.; Grządziel, L.; Bodzenta, J.; Szuber, J. Comparative Study of Surface Morphology of Copper Phthalocyanine Ultra Thin Films Deposited on Si (111) Native and RCA-Cleaned Substrates. *Thin Solid Films* **2012**, *520*, 3965−3970.
(44) Celler, G. K.; Barr, D. L.; Rosamilia, J. M. Etching of Silicon by the RCA Standard Clean 1. *Electrochem. Solid-State Lett.* **2000**, *3*, 47−49.
(45) Williams, R.; Goodman, A. M. Wetting of Thin Layers of SiO_2 by Water. *Appl. Phys. Lett.* **1974**, *25*, 531−532.
(46) Wenzel, R. N. Resistance of Solid Surfaces to Wetting by Water. *Ind. Eng. Chem.* **1936**, *28*, 988−994.
(47) Vlerken, L.; Vyas, T.; Amiji, M. Poly(ethylene glycol)-Modified Nanocarriers for Tumor-Targeted and Intracellular Delivery. *Pharm. Res.* **2007**, *24*, 1405−1414.
(48) Halperin, A. Polymer Brushes That Resist Adsorption of Model Proteins: Design Parameters. *Langmuir* **1999**, *15*, 2525−2533.
(49) Carignano, M. A.; Szleifer, I. Prevention of Protein Adsorption by Flexible and Rigid Chain Molecules. *Colloids Surf., B* **2000**, *18*, 169−182.
(50) Singh, N.; Cui, X.; Boland, T.; Husson, S. M. The Role of Independently Variable Grafting Density and Layer Thickness of Polymer Nanolayers on Peptide Adsorption and Cell Adhesion. *Biomaterials* **2007**, *28*, 763−771.
(51) Steels, B. M.; Koska, J.; Haynes, C. A. Analysis of Brush-Particle Interactions Using Self-Consistent-Field Theory. *J. Chromatogr. B: Biomed. Sci. Appl.* **2000**, *743*, 41−56.
(52) Bartucci, R.; Pantusa, M.; Marsh, D.; Sportelli, L. Interaction of Human Serum Albumin with Membranes Containing Polymer-Grafted Lipids: Spin-Label ESR Studies in the Mushroom and Brush Regimes. *Biochim. Biophys. Acta, Biomembr.* **2002**, *1564*, 237−242.
(53) Di Lullo, G. A.; Sweeney, S. M.; Körkkö, J.; Ala-Kokko, L.; San Antonio, J. D. Mapping the Ligand-Binding Sites and Disease-Associated Mutations on the Most Abundant Protein in the Human, Type I Collagen. *J. Biol. Chem.* **2002**, *277*, 4223−4231.
(54) Murthy, R.; Shell, C. E.; Grunlan, M. A. The Influence of Poly(ethylene oxide) Grafting via Siloxane Tethers on Protein Adsorption. *Biomaterials* **2009**, *30*, 2433−2439.
(55) Frederix, F.; Bonroy, K.; Reekmans, G.; Laureyn, W.; Campitelli, A.; Abramov, M. A.; Dehaen, W.; Maes, G. Reduced Nonspecific Adsorption on Covalently Immobilized Protein Surfaces Using Poly(ethylene oxide) Containing Blocking Agents. *J. Biochem. Biophys. Methods* **2004**, *58*, 67−74.
(56) Yang, S. Y.; Mendelsohn, J. D.; Rubner, M. F. New Class of Ultrathin, Highly Cell-Adhesion-Resistant Polyelectrolyte Multilayers with Micropatterning Capabilities. *Biomacromolecules* **2003**, *4*, 987−994.
(57) Moore, E.; Delalat, B.; Vasani, R.; Thissen, H.; Voelcker, N. H. Patterning and Biofunctionalization of Antifouling Hyperbranched Polyglycerol Coatings. *Biomacromolecules* **2014**, *15*, 2735−2743.
(58) Kurkuri, M. D.; Driever, C.; Johnson, G.; McFarland, G.; Thissen, H.; Voelcker, N. H. Multifunctional Polymer Coatings for Cell Microarray Applications. *Biomacromolecules* **2009**, *10*, 1163−1172.
(59) Hook, A. L.; Thissen, H.; Voelcker, N. H. Advanced Substrate Fabrication for Cell Microarrays. *Biomacromolecules* **2009**, *10*, 573−579.